FEM STUDY OF THE CONTACT AREA AND PRYING ACTION IN T-STUB STEEL CONNECTION

Luciano Mendes Bezerra
Universidade de Brasília, UnB – Brasília, DF
lmbz@unb.br

Cleirton André Silva de Freitas
Universidade de Brasília, UnB – Campus Universitário Darcy Ribeiro, Bloco SG12, Brasília, DF, 70910-900
andrefreitas@unb.br

Yosiaki Nagato
Universidade de Brasília, UnB – Brasília, DF

Abstract: *This paper presents a numerical study of T-stub steel connections using FEM analyses. Depending on the thickness of the flange, a T-stub steel connection may be classified as rigid, semi-rigid, or flexible. In such connections prying action phenomenon may take place. For rigid flanges no praying action is observed. For flexible flanges praying action may overload the bolts. Prying action effect on the bolts has been studied before but the location of the prying action forces has always been simplified. A better knowledge of the contact stresses between T-stub flange and support base is helpful in understanding the appropriate resistance mechanism of the T-stub connections. Contact area between T-stub and support base depends largely on the thickness of the flange. The effect of the thickness of T-stub flanges on contact areas between flanges and support base is investigated in this paper. A 3D finite element model is used and interface elements are employed for the investigation. Nonlinear FE analyses are undertaken on connection with different flange thickness and bolt preload. Nonlinear gap elements are used as interfaces. Discussion and conclusions on contact areas and stresses, prying action distributions, resultant of loads on bolts, and the resistance of the T-stub connections are presented.*

Keywords*: T-stub connections, contact stresses, prying action, stresses on bolts*

1 - Introduction

T-stubs are connections usually linking tension members to beams. Studies [Kulak et al, 2001] show that bolts connecting this type of connection to a support base may be under high stresses due to a phenomenon called “prying action”. This phenomenon is associated to the flexural rigidity of the T-Stub flange. For very rigid flanges no prying action is detected. Prying action is a physical phenomenon due to the eccentricity between applied external force and the line of resisting bolts [Ribeiro, 1998]. Prying action increases the forces acting over the bolts and, therefore, must be considered for a correct design of T-Stub connections [Galambos, 1996].

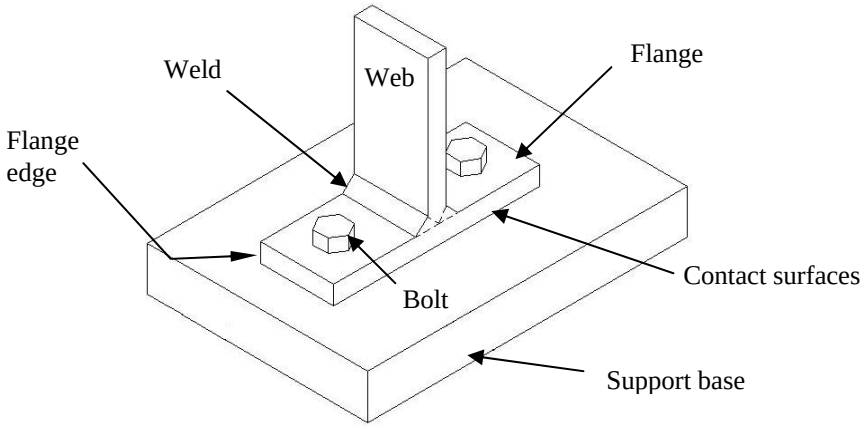

Figure 1 – T-stub steel connection

According to Kulak [Kulak et al, 2001], an external applied load in the T-stub connection with preload on the bolts reduces the contact pressure between the T-stub flange and the support base. However, depending on the flexural rigidity of this flange, additional contact forces, known as the "prying action", may be developed between flange and support base (Figure-1). By equilibrium, such prying action forces produce additional loads on the bolts. Analytical models for the design of T-stub connection, proposed by Douty and McGuire [Douty and McGuire, 1965], Struik and deBack [Struik and deBack, 1969], and Nair [Nair, Birkemoe and Munse, 1969], consider the

prying action forces concentrated at a line at the edge of the T-stub flanges. This approach has been adopted by many Standards [ASCE,1971, Brazilian Standard for Steel Construction, NB-14, 1986, and Brazilian Manual]. Work published by Leon [Leon, Swanson and Kokan, 2001] shows qualitatively the distribution of the prying action forces on the contact area between the T-stub flange and the support base (Figure-1).The characterization of the position of the resultant of contact force (RCF) between flange and support base (Figure-1) may influence the way engineers model T-stub connections. The knowledge of the contact forces (or stresses) between T-stub flange and support base gives a more precise location of the prying action force. This prying force location may be taken into account in more realistic analytical models for the design of T-stub connections. This paper is part of a research under progress at the University of Brasilia for the numerical verification of the behavior of T-stub steel connectors [Freitas, 2004].

2 – The T-stub steel connection to study

The objective of the current article is the numerical investigation of the influence of the T-stub flange thickness on the prying action forces, how these forces are distributed between the T-stub flange and the support base, and the extra loading on the bolts (See Figure-1). All the investigations reported in this article are based on numerical experimentation taken on the T-stub model represented in Figure-2. The T-Stubs considered in this study have flange of 50x140(mm) with ½" web and two bolts (Figure-1 and 2). Different T-stubs with varying flange thickness are studied For the numerical analyses, finite element (FE) models (P1D to P5D) as reported in Table-1 are considered. Figure-2 shows the T-stub connector with bolt hole diameters of 14mm and distances to the flange edges according to the recomemdations of NBR8800/86. For such range of thickness the prying action variation is studied. This artcle is limited to the simple case of T-stubs with two holes. The web thickness of all T-stub connectors is 1/2". The weld connecting the T-stub web and the flange is a 6mm weld as shown in the Figure-2. The material properties for the connections are Modulus of Elasticity, E=205000MPa, and Poisson's ratio ν=0,3. The lengths of the bolts are appropriate for the lab tests (lab tests are not under the scope of this article). Therefore, the length of the bolts is 114,3mm (4,5").

Table 1: T-stub dimensions and flange thicknesses.

Order	Model	Thickness (t_f)	
		Inch	Millimeter
01	P1D	1/2 "	12,7
02	P2D	3/8 "	9,5
03	P3D	5/16 "	7,9
04	P4D	1/4 "	6,4
05	P5D	3/16 "	4,8

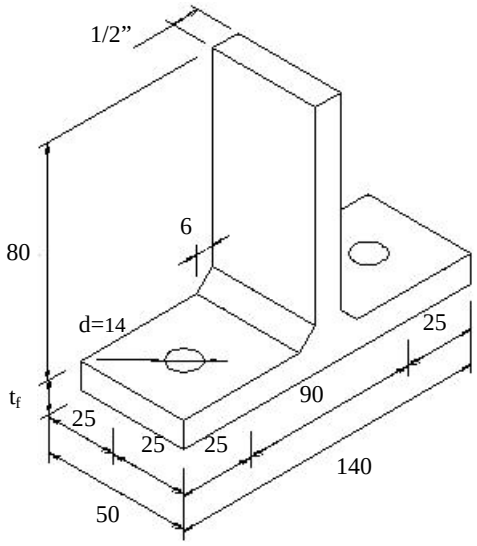

Figure 2 – T-stub dimensions (mm or inches)

3 – The solid 3D finite element model

The finite element program ANSYS is used for all the numerical investigation undertaken in this work. All the FE-models employed the solid element SOLID45. This is an isoparametric finite element with 8 nodes and 3 degrees of freedom (translation in X, Y and Z directions) per node. The FE-model has 776 solid elements and 2141 nodes employed for the discretization of each of the five models listed in Table-1. All the FE-models have the same mesh but different element thickness for the flanges. A perfect link is assumed in the interface between the head of the two bolts and the T-stub flange. The FE mesh is shown in Figure-3.Interface elements are placed in the FE-models in the position in between the support base and T-stub flange (Figure-1) simulating the contact between the flange and the support base. These elements have the purpose to catch the contact areas and contact forces between the T-stub flange and the support base. The element GAP3D from the ANSYS element library is selected as the interface element. GAP3D is a one-dimensional, point-to-point, contact element with three degrees of freedom (translation in X, Y and Z directions) per node and the ability to withstand only compression forces in the direction normal to the surfaces. Although the interface element has the ability to consider friction between two surfaces, in this study friction is not taken into account. GAP3D elements are defined as connecting two nodes, one node at the node grid in the inferior face of the flange and the other node located at a corresponding node grid placed underneath the flange. The interface GAP3D are represented as lines and pointed out in Figure-3. The compression

stiffness property of the interface elements is made very high simulating a very rigid support base where the T-stub connection is fixed. A total of 333 GAP3D elements are used - see Figure-3.

4 – Loads and boundary conditions

In Figure-4, a cross section of the FE-model is illustrated. The applied load and the constraints are also represented in that figure. Figure-4 brings another view of the FE-model including the bolts and the lines representing the interface elements. Longitudinal displacement of the bolts is allowed along the bolt length. In the interface elements one node is fixed at the T-stub flange node and the other node is anchored at the base - simulating a rigid support base. The interface elements are distributed along the grid of nodes as shown in Figure-5. The contact between T-stub flange and support base bears the preload on the bolts and the "prying" action produces by the pulling load at the web. For the current study, the loads applied on the bolts distinguish two "load cases" named "Case-1" and "Case-2". Case-1 has no preload, but in Case-2 a preload on the bolts is applied before the external pulling load on the web is applied. In the FE-models it is important to apply the loads in the sequence as carried out in practice. In Case-1, where no preload on the bolts is prescribed, the FE-models are submitted exclusively to the pulling load on the web (see Figure-4). In Case-2, the preload on the bolts is first applied, and, subsequently, the external pulling load is applied on the nodes of the web. In all analyses, the external pulling load is increased monotonically in four load steps, begining at 40kN and going up to 160kN (in increments of 40kN). When no preload exists, the external load is applied in the first four load steps. When there is preload on the bolts, the first load step is the preload; and the subsequent four load steps are the external pulling load. In Case-2 a total of five load steps is necessary while in Case-1 just four. The external load on the web is uniformly applied over all the nodes at the top (see Figure-4). The loads and preloads associated with each load case are summarized in Table-2.

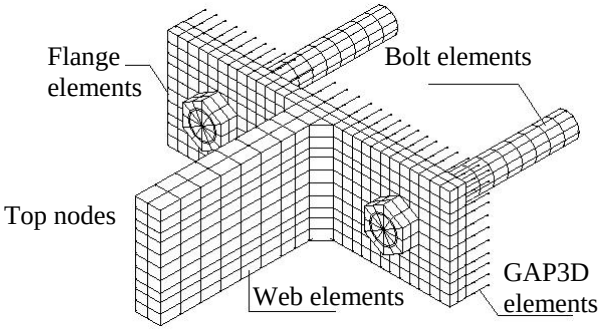

Figure 3 – Complete Mesh for T-stubs: P1D, P2D, P3D, P4D, and P5D

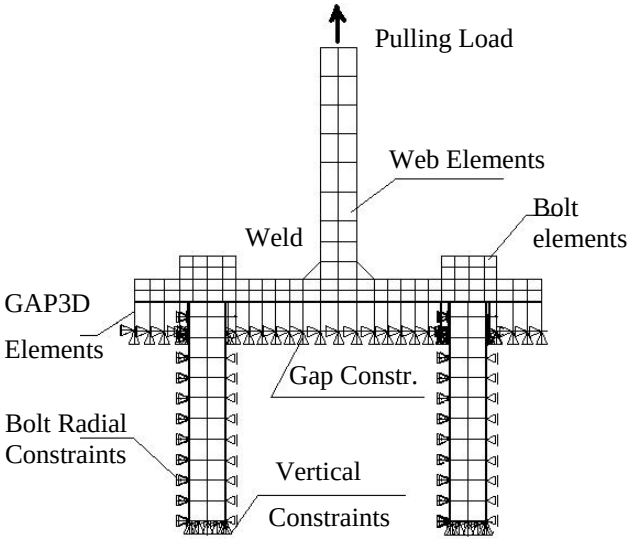

Figure 4 – FE mesh with interface and boundary

Table 2: Loading cases (LC), bolt preloads, and pulling load steps (LS)

FE Models	LC	Load Steps (LS)	Preloads	Level of Pulling LS (kN)
5 FE models with 2 bolts	Case-1	4 LS	0.00	40 – 80 – 120 - 160
	Case-2	5=1Preload+4LS	45 kN	40 – 80 – 120 - 160

5 – Numerical results for the distribution of the contact forces

For the numerical results, the identification of node grid at the interface between flange and support base as illustrated in Figure-5 is assumed. The grid represented by letter A to L and numbers 1 to 10 is made of regular squares of approximate 5mm in size.The longitudinal "L" direction is represented by the L-Axis and the transversal direction by the T-Axis. Three parameters are examined from the numerical outputs: Distribution in the flange of the contact forces, Resultant of the contact forces and their locations, and Resultant of forces acting on the bolts.

5.1 – Contact forces for Case-1

Figure-6 presents the magnitudes and distributions of the contact forces between the surfaces of the T-stub flange and the rigid support base for Case-1. The values of the contact force are directly taken from the interface elements. Note that the pulling load on the web is applied in four load steps for Case-1. Therefore, plots in the

columns of Figure-6 refer to load levels - see note on the top left corner of every plot. Plots in the same line are related to a particular flange thickness as specified in Table-1.

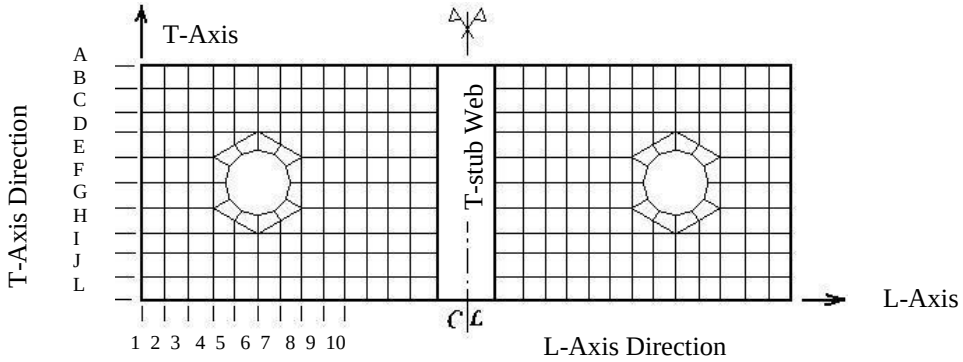

Figure 5 – Identification of axis and nodes in the grid

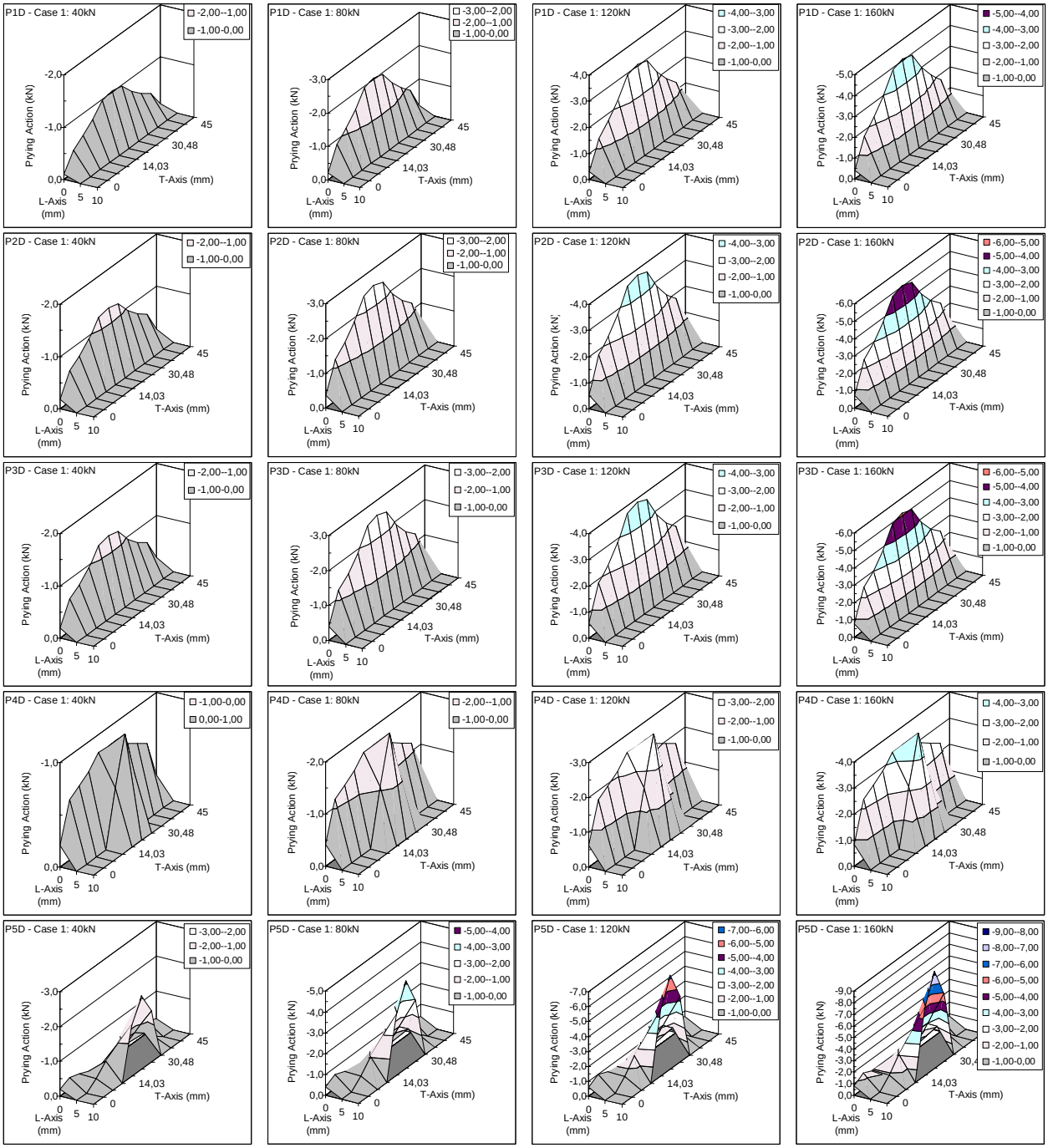

Figure 6 – 3D-dimensional distribution of prying action for Case-1 (no-preload on the bolts)

To save space in Figure-6, T-Axis is limited to the range [0, 10] - where contact forces are significant. Note that the hole of the bolt starts at 18mm from the edge of the flange (25-14÷2, see Figure-2). In Figure-6, despite the nolinearity caused by the presence of the interface elements, the analyses generate plots (for a given flange thikness) proportional to the load level.

5.2 – Contact forces for Case-2

For Case-2, the nonlinerity due to the interface elements is more noticeable. Observe that in the start of the analysis, the preloads on the bolts are applied and this preload squeezes the flange against the support base. When the external pulling load starts to take action on the web, the contact forces (generated by the bolt preload) begins to decline. Note that, in this case, the pulling load on the web is applied in four subsequente load steps only after the first load step has been accomplished, which corresponds to the application of the bolt preload.

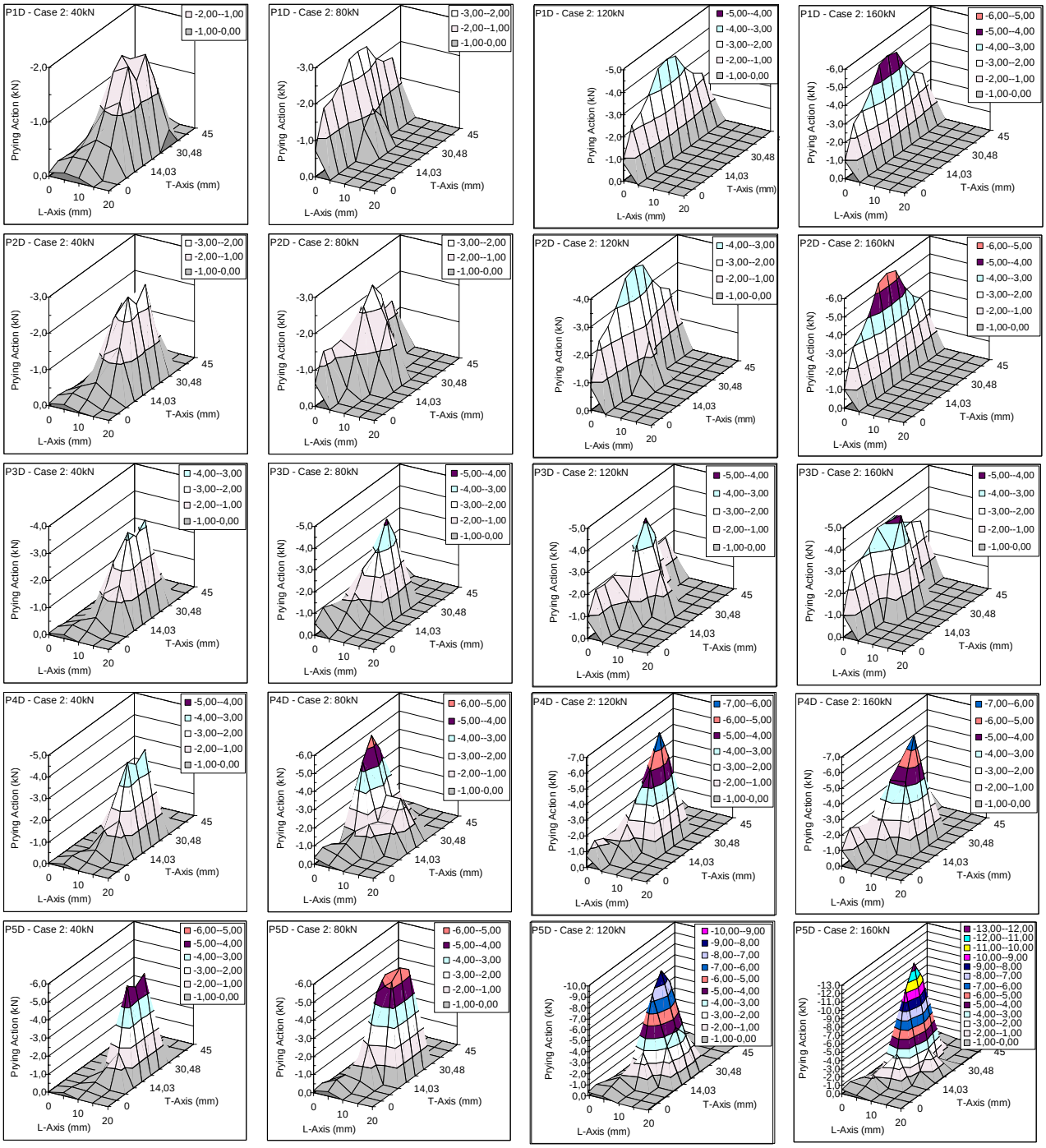

Figure 7 – 3D-dimensional distribution of prying action for Case-2 (preloads on the bolts)

Figure-7 shows the magnitude and distribution of the contact forces between the surface of the T-stub flange and the rigid support base for Case-2. As in Case-1, the values of the contact force are taken directly from the

interface elements In Figure-7, as before, plots in the same column refer to a specific load level, and plots in the same line of the figure are related to a particular flange thickness (Table-1). To save space in Figure-7, the plots are limited to the range [0,10] of the L-Axis, range where contact forces are significant. Remember that bolt´s holes start at 18mm from the edge of the flange (25-14÷2, Figure-2)

5.3 – Resultant of contact forces on the T-stub flanges

The analysis of the contact forces in Figures 6 and 7 shows that thinner flanges give rise to larger contact forces. This confirms what is in the literature [Kulak et al, 2001] and is clear Figures 8 and 9. Figure-8 is associated to Case-1 (no preload on the bolts) and Figure-9 is related to Case-2 (preload on the bolts). Such figures plot the resultant of contact forces (RofCFs) as function of flange thickness. Due to symmetry, the RofCF value is the sum of all contact forces on just one side of the flange. The RofCF grows with the decrease in thickness. The negative sign is assotiated to the compressive forces between flange and support base.

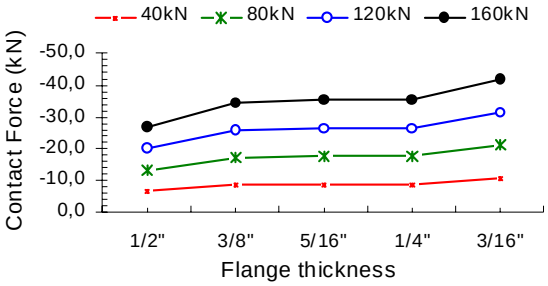

Figure 8 – Variation of RofCFs with flange thickness for Case-1

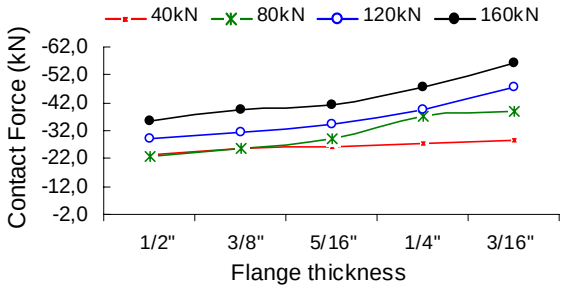

Figure 9 – Variation of RofCFs with flange thickness for Case-2

5.4 –Distribution and location of contact forces on T-stub flanges

The ouline of the contact force distribution along the transversal (T-Axis) direction can be seen in Figures 10 to 12, and Figures 13 to 15, respectively, for Case-1 and Case-2. Those pictures were done based on Figures 6 and 7. Figures 10 and 11, shows the distribution of the RofCFs along the T-Axis direction, respectively, for flange thicknesses of 1/16" (thin flange P5D) and 1/2" (thick flange P1D). These RofCFs are found as the sum of contact forces along L-Axis corresponding to a particular letter (transversal position). For example, in Figure-10, at load level 160kN, the RofCF of -12kN (corresponding to letter F) is the sum of all contact forces at points F-1, F-2, and F-3 (along L-Axis) at the grid defined in Figure-5.

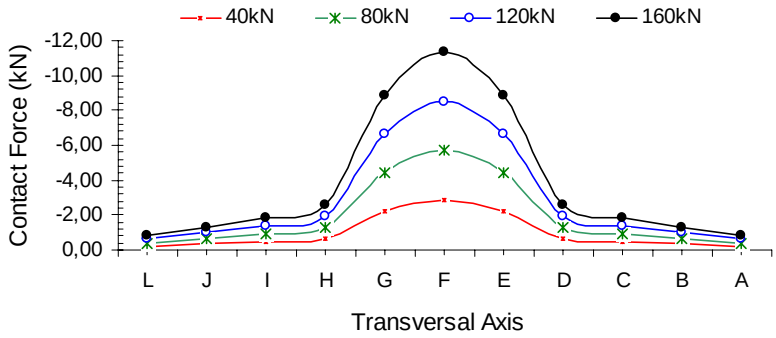

Figure 10 – Resultant prying forces along the transversal axis for P5D (Case-1)

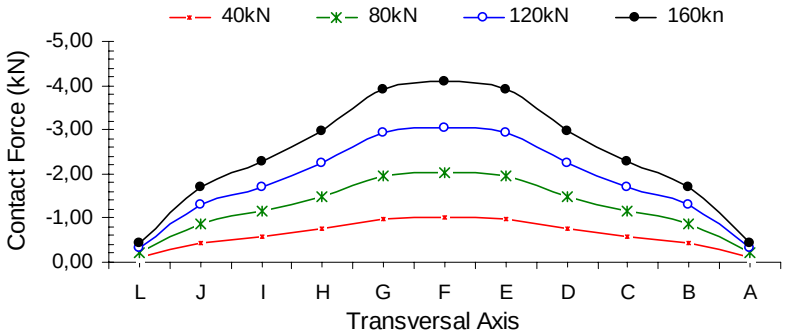

Figure 11 – Resultant contact forces along T-Axis for P1D (Case1)

Observing Figures-10, note that the RofCFs are more concentrated near the bolt head when the flange is thin. In Figure-11, for a thicker flange the RofCFs are less concentrated and spread over the T-axis. To save space, only the plots correspond to the thinnest and the thickest flange is shown in Figures 10 and 11, respectively. Figure-12 summarizes the distribution and magnitude of the RofCF for the flange thicknesses considred and for the load level of 160kN. Figures 13, 14, and 15 are the equivalent figures for Case-2. In theses figures the RofCFs are higher than in Figures-10, 11 and 12, and it is due to the preload on the bolts. For the L-Axis direction, Figure-16 and 17 illustrate the variation with the thickness of the distribution and magnitude of the RofCFs for Cases 1 & 2, respectively, when the pulling load is at 160kN.

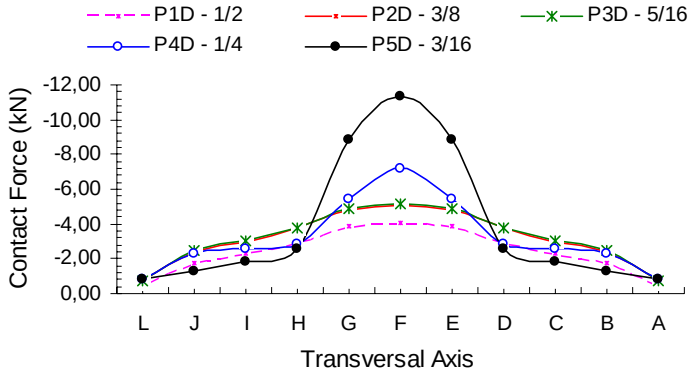

Figure 12 – Resultant contact forces along T-Axis for 160kN (Case1)

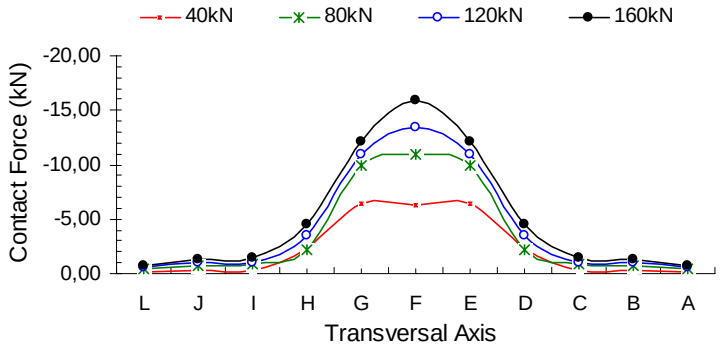

Figure 13 – Resultant contact force along the T-Axis for P5D (Case-2)

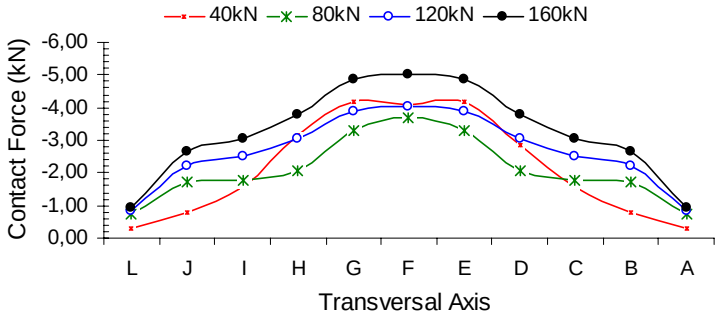

Figure 14 – Resultant contact force along the T-Axis for P1D (Case-2)

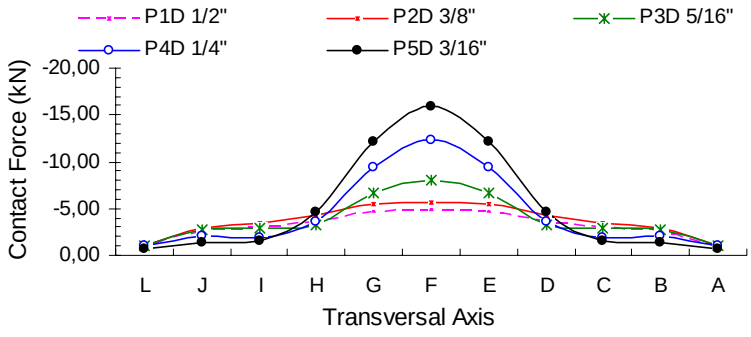

Figure 15 – Resultant contact forces along T-Axis for 160kN (Case-2)

In Figure-16, it is noticeable that when no preload is applied (Case-1) the contact forces are concentrated at position-1 (edge of the flange in Figure-5). This is applicable for the thicker flanges P1D, P2D and P3D. Still in Figure-16, for the thinner flanges, P4D and P5D, the distribution of contact forces are quite different; the contact forces do not concentrate along the flange edge (origin of L-Axis). For P4D, the contact force distribution decreases from the edge towards the bolt line (position-3, along T-axis, in Figure-5), and for the thinnest flange, P5D, the RofCF distribution increases towards the bolt line. Note that, the RofCFs are at 1,16mm and 6,57mm from the edge of the flange, respectively, for P4D and P5D T-stubs. With respect to Case-2, a significant change can be noticed in the distribution of the contact forces in the longitudinal direction. Due to the preload on the bolts, the flanges of the T-stubs have contact areas larger than in Case-1. The contact forces, in Case-2, depend on the rigidity of the flange and on the external applied load on the web.

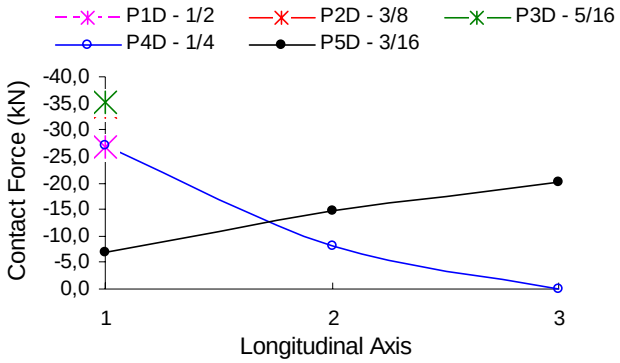

Figure 16 – Contact force along the L-Axis for 160kN (Case-1)

Table 3: Resultants of the contact forces of Case-2

	P1D - 1/2"		P2D - 3/8"		P3D - 5/16"		P4D - 1/4"		P5D - 3/16"	
Load Step.	Position.	Load.	Position.	Load.	Position.	Load.	Position.	Load.	Position.	Load.
40kN	10,30	-2,35	11,90	-2,58	12,66	-2,65	13,55	-2,74	14,61	-2,83
80kN	0,57	-2,29	3,10	-2,59	5,76	-2,91	6,95	-3,74	11,80	-3,91
120kN	0,00	-2,90	0,39	-3,16	2,53	-3,43	6,22	-3,97	10,29	-4,77
160kN	0,00	-3,57	0,00	-3,97	1,21	-4,14	5,04	-4,77	9,22	-5,64

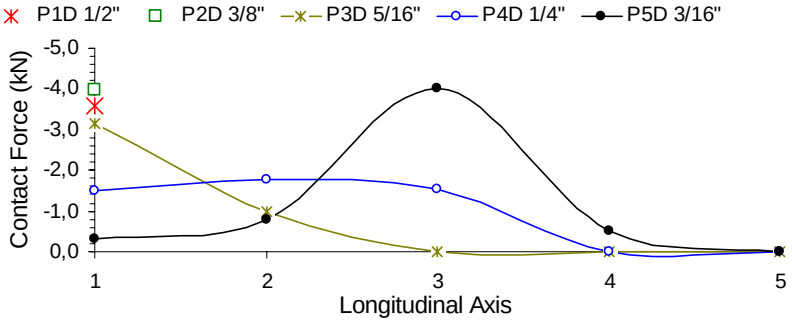

Figure 17 – Contact force along the L-Axis for 160kN (Caso-2)

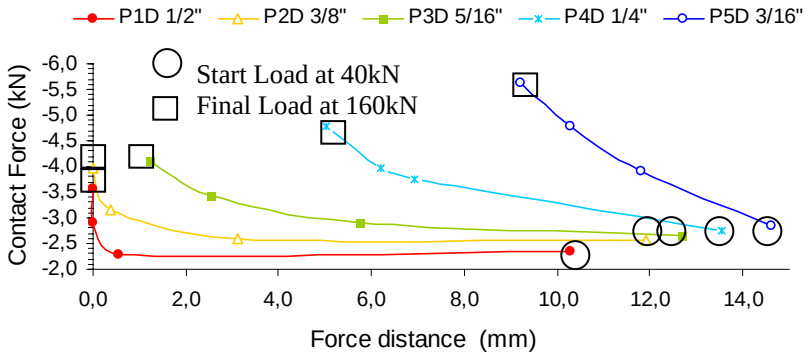

Figure 18 – Contact force resultant and force distance to flange edge (Case-2)

Figure-17, for the load level of 160kN, presents the distribution of contact forces for Case-2. Table 3, shows the magnitude and location of the RofCFs in Case-2 and the corresponding plots are shown in Figure-18. In the

beginning, see Table 3 and Figure-18, for thinn flanges the RofCFs are closer to the bolt heads than for thick flanges. As the external load increases, the location of the RofCFs changes. For T-stubs P1D and P2D, and load level of 160kN, the contact forces travel to the edge of the flange. For the other T-stubs, there is also a move on the location of the RofCFs towords the edge. The positions of the RofCFs can be observed in Table 3 and in Figure-18.

Fgure-19 presents the distance of the RofCFs to the flange edge for each flange thickness and for different load levels. For small load levels the curve is practically lineal. With the gradual increase of the load, the curve is non-linear. Note that, for 120kN and 160kN, and thicker flanges (larger rigidity), the position of the RofCFs is at the edge of the flange - as adopted in the traditional models for prying action in T-stubs. The variation of the position of the RofCFs can be visualized in Figure-20.

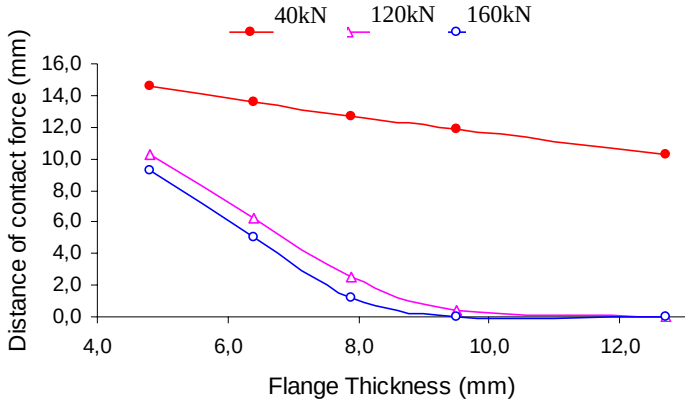

Figure 19 – Distance of the RofCFs to flange edge vs. flange thickness (Case-2)

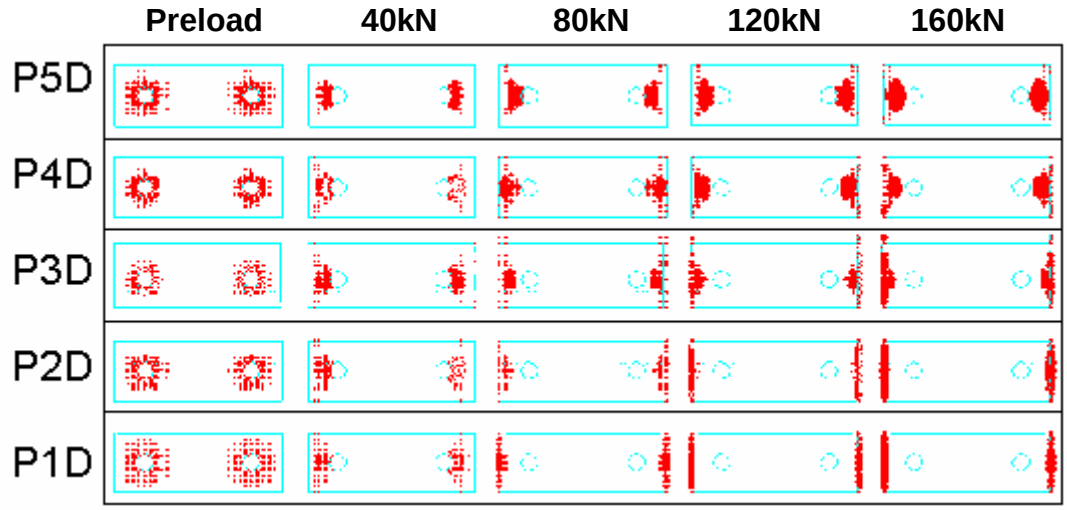

Figure 20 – Evolution of the contact force distributions for Case-2

5.5 – Force on the bolts in the T-stub connetions

From the analyses undertaken in this article, the force on the t-stub bolt varies with the flange thicknesses. For the sake of simplicity, we call “FonB” as the force acting on the t-stub bolt. For the range of flanges considered in this reseach (see Table-1), the analyses confirm that the thinner the flange, the larger the force on the bolt.

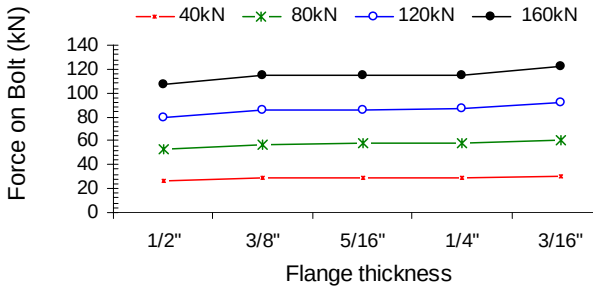

Figure 21 – Relationship of the bolt force and the flange thickness (Case-1)

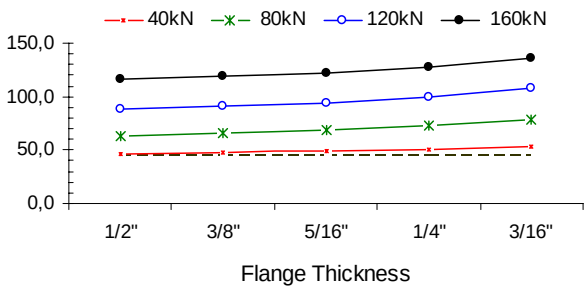

Figure 22 – Relationship of the bolt force and the flange thickness (Case-2)

The variation of the "FonB" as function of the flange thicknesses is represented in Figure-21 for Case-1, and in Figure-22 for Case-2. For the T-stub connection P1D and P5D (ends of Table-1), the relation between "FonB" in Case-2 and in Case-1 may be seen Figure-23. The other cases are inbetween the two plots. Note that the intensity of the FonB in Case-2 is greater than in Case-1.

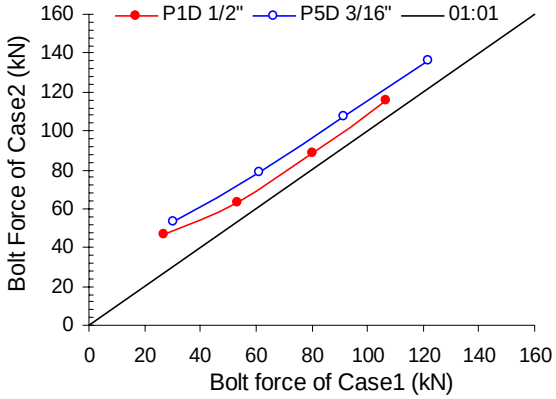

Figure 23 – Relation between the RofCFs in Case-2 and in Case-1

6 – Conclusion

From the numerical results presented, considering the range of T-stub flange thicknesses (in Table-1), some conclusion may be drawn. a) The value of the prying force on the bolts depends on the level of applied load in the web of the T-stub, on the flexural rigidity of the flange, and, consequently, on the flange thickness. b) In the longitudinal direction (L-Axis in Figure-5), the position of the Resultant of Contact Forces (RofCFs) (and, thus, the prying force) is not always at the edge of the flange as supposed by many simplified models adopted in the literature. c) The position of the RofCFs relies on the flange thickness of the T-stub connection, on the amount of applied load, and on the preload given on the bolts. d) In the transversal direction, the position of the prying force is in the vicinity to the head of the bolt. e) The force on the bolt depends on the applied load and on the flexural rigidity of the flange.

7 – Acknowledgements

This article is part of a research in progress at University of Brasilia. The authors want to express their gratitude to FINATEC (Fundação de empreendimentos científicos e tecnológicos), CNPq (The Brazilian National Council for Scientific and Technological Development) and to CAPES (the Brazilian Committee for Postgraduate Courses in Higher Education) for the financial supports.

8 – Reference

Kulak, G. L., Fisher, J. W., Struik, J.H.A.. 2001. Guide to Design Criteria for Bolted and Riveted joints, American Institute of Steel Construction, Chicago.

Galambos, T. V.. 1996. Basic steel design with LRFD. Prentice Hall, Upper Saddle River, New Jersey.

Ribeiro, L. F. L.. 1998. Estudo do comportamento estrutural de ligações parafusadas viga-coluna com chapa de topo. Tese de Doutorado. Escola de Eng. de São Carlos, USP.

Leon, R.T.; Swanson, J.A.; Kokan, D.S.. 2001. Advanced finite element modeling of bolted T- stub connection components. Journal of Construction Steel Research.

Freitas, C. A. S. 2004. Study of T-stub Connections - Technical Report. Universidade de Brasília, UnB.

Douty, R. T.: McGuire, W. 1965. High Strength Bolted Moment Connections. Journal of the Structural Division. ASCE, Vol.91, ST2.

Struik, J.H.A.; deBack,J.. 1969. Tests on Bolted T-stub with respect to a Bolted Beam-to-Column Connections. Report 6-69-13, Stevin Laboratory, Detf University of Technology, Detf, the Netherlands

Nair, R. S.; Birkemoe, P. C.; Munse, W. H.. 1969. High Strength Bolts Subjected to Tension and Prying. Structural Research Series 353. Departament of Civil Engineering, University of Illinois, Urbana.

ASCE. 1971. Commentary on Plastic Design. Manual 41, New York.

Norma Brasileira, NB-14. 1986. Projeto e execução de estruturas de aço de edifícios – Associação Brasileira de Normas Técnicas, ABNT, Rio de Janeiro.

9 – Responsibility notice

The author(s) is (are) the only responsible for the printed material included in this paper.